Review of the Learning-based Camera and Lidar Simulation Methods for Autonomous Driving Systems

Hamed Haghighi[1], Xiaomeng Wang[1], Hao Jing[1], and Mehrdad Dianati[2]

Abstract—Perception sensors, particularly camera and Lidar, are key elements of Autonomous Driving Systems (ADS) that enable them to comprehend their surroundings for informed driving and control decisions. Therefore, developing realistic camera and Lidar simulation methods, also known as camera and Lidar models, is of paramount importance to effectively conduct simulation-based testing for ADS. Moreover, the rise of deep learning-based perception models has propelled the prevalence of perception sensor models as valuable tools for synthesising diverse training datasets. The traditional sensor simulation methods rely on computationally expensive physics-based algorithms, specifically in complex systems such as ADS. Hence, the current potential resides in learning-based models, driven by the success of deep generative models in synthesising high-dimensional data. This paper reviews the current state-of-the-art in learning-based sensor simulation methods and validation approaches, focusing on two main types of perception sensors: cameras and Lidars. This review covers two categories of learning-based approaches, namely raw-data-based and object-based models. Raw-data-based methods are explained concerning the employed learning strategy, while object-based models are categorised based on the type of error considered. Finally, the paper illustrates commonly used validation techniques for evaluating perception sensor models and highlights the existing research gaps in the area.

Index Terms—Learning-based, deep generative models, perception sensor models, image synthesis, 3D point cloud synthesis, camera, Lidar, autonomous driving systems, simulation.

I. INTRODUCTION

THE development and validation of Autonomous Driving Systems (ADS) includes several techniques drawn from computer vision, machine learning, motion planning, simulation, civil engineering, robotics, and more. Safety is a critical concern in ADS, with the potential for severe consequences in the event of a system failure, as evidenced by recent crashes involving Uber and Tesla [72], [70]. The physical testing of ADS, while valuable, poses challenges in terms of time, labour, and cost, requiring extensive driven miles to statistically prove safety [36]. Moreover, certain dangerous scenarios may not be feasible or ethical for real-world testing. In contrast, virtual testing through a simulation environment offers numerous advantages by allowing the efficient simulation of a significant number of miles in a short time, testing safety-critical scenarios without physical damage, and modelling complex and costly-to-recreate traffic scenarios.

In the domain of ADS applications, perception sensors, including cameras and Lidar, play a pivotal role. These sensors monitor the surrounding environment, detecting moving objects such as vehicles, cyclists, pedestrians, and stationary objects such as traffic lights and road signs. It is critical to test ADS with the realistic performance of the perception sensors, especially in challenging environments where their performances are likely to be degraded. Hence, the creation of realistic sensor models becomes vital, facilitating extensive testing and validation in simulated environments and contributing to the overall safety and reliability of ADS.

The surge in deep learning-based models for autonomous driving [24], especially in perception applications, has led to a substantial demand for annotated sensory datasets to train these models. For this reason, numerous sensory datasets have been recorded from real driving scenes [41] and have been annotated by human labour in recent years. However, the process of collecting and annotating real-world datasets is costly and presents challenges such as privacy concerns and safety hazards. As a solution, many researchers have turned to simulation environments to generate synthetic datasets. Simulation frameworks enable the rapid creation of extensive sensory data with ground-truth annotations and the generation of edge-case scenarios without posing safety hazards. These synthetic datasets are either used in conjunction with real datasets to train perception models or employed independently with domain adaptation techniques. In both scenarios, realistic simulation of perception sensors plays a significant role in enhancing the performance of downstream perception tasks.

The literature on sensor simulation presents two fundamental approaches: physics-based and learning-based techniques [63]. Physics-based methods involve explicit simulations of sensor-related physical phenomena, relying on intricate hand-crafted formulations for approximations. For instance, Liu et al. [42] introduced a high-fidelity physics-based camera model for autonomous driving, incorporating components that precisely simulate light propagation, surface materials, camera lens, and aperture. Although capable of generating high-fidelity sensor images, such systems require extensive computations. In contrast, learning-based models have gained popularity in recent years to address the complexity of physics-based models. Unlike physics-based approaches, learning-based methods leverage statistical models to implicitly uncover underlying relations by learning from data. The growing

[1]H. Haghighi, X. Wang, and H. Jing are with WMG, University of Warwick, Coventry, U.K. (Corresponding author: Hamed.Haghighi@warwick.ac.uk)

[2]M. Dianati is with the School of Electronics, Electrical Engineering and Computer Science at Queen's University of Belfast and the WMG at the University of Warwick.

availability of real-world recorded perception sensory datasets, coupled with the success of deep generative models in synthesising high-dimensional sensory data, has led to a rapid expansion of the literature on learning-based sensor models.

This article aims to review the state-of-the-art learning-based perception sensor simulation and validation techniques. The simulation approaches are discussed within the framework of two categories: raw-data-based and object-data-based sensor models. While raw-data-based models focus on generating the raw sensory, e.g. camera RGB image or Lidar point cloud, object-based models approximate the perceived object properties, e.g. bounding boxes. Raw-data-based models are mainly used for testing or training downstream perception models, whereas object-based models find application in subsequent planning and control models. We categorise the perception sensor model validation techniques into qualitative and quantitative approaches. Qualitative approaches rely on the visualisation of sensor model output or a downstream component's output. On the other hand, quantitative techniques use various mathematical metrics to measure sensor model performance.

In the context of autonomous driving simulation, several literature review papers have explored aspects including driving simulation frameworks, synthetic datasets, and sensor simulation approaches. For instance, Rosique et al. [61] conducted a review of perception systems and simulators for ADS, emphasising characteristics of sensor hardware and simulators used in vehicle tests, game engines, and robotics for ADS testing. Kang et al. [37] provided an overview of public driving datasets and virtual testing environments, focusing on accessible virtual testing environments for closed-loop ADS testing. Schlager et al. [63] conducted a study reviewing perception sensor models, categorising radar, Lidar, and camera models based on fidelity levels. In a recent work [15], the authors concentrated on reviewing digital camera components and their simulation approaches in the context of ADS and robots. Despite the coverage of various sensor simulation methods, there is a noticeable gap in the discussion of state-of-the-art learning-based methods, particularly those based on recent deep generative models. Furthermore, existing research has not adequately explored sensor simulation validation approaches, a crucial aspect for virtual verification and validation of ADS.

The summary of our paper's contributions is as follows:

- A comprehensive literature review of the learning-based camera and Lidar simulation methods is carried out, with a specific emphasis on the latest techniques rooted in deep generative models.
- A novel perspective toward learning-based perception sensor simulation is discussed, exploring both unsupervised and supervised learning approaches.
- A detailed explanation and categorisation of validation approaches for learning-based perception sensor models are provided.

The rest of the paper is organised as follows. Section II provides a detailed explanation of the working mechanism of the camera and Lidar sensors, as well as the concept of sensor simulation. Section III explores and categorises the state-of-the-art learning-based models. Section IV presents various methods for validating perception sensor models. Finally, Section V provides a concluding remark for the paper, and identifies research gaps.

II. PERCEPTION SENSORS AND SIMULATION METHODOLOGIES

This section explores the characteristics and measurement disturbances of camera and Lidar sensors in the context of ADS applications. Additionally, it aims to clarify the concept of "sensor simulation/modelling" and different perspectives towards simulation approaches.

A. Characteristics and Mechanism

The perception sensors can be regarded as a system that receives environmental signals as input and processes them into interpretable data. The input signals can be acquired through active scanning methods such as Lidar or passive sensing techniques like those employed by cameras. The output interface data includes human-understandable information, e.g. RGB images from camera or point clouds from Lidar. We separately explain the functionality and characteristics of the camera and Lidar sensors in the subsequent paragraphs.

1) Camera Sensor: The process of camera image generation is depicted in Fig. 1. Cameras operate as passive sensors since they do not emit signals for measurements but instead rely on graphic processing to sense the environment. Particularly, light sources (e.g. sun and electric lighting) generate the rays of light which pass through the media, e.g. air, water, cloud, rain, fog, snow, etc., and strike surfaces of different objects, such as vehicles, pedestrians, buildings, roads and vegetation. The light then reflects from the surfaces, travels through the media and reaches the camera. The rays of light from the scene pass through the camera lens first and then reach the image sensor (CCD or CMOS). The image sensor then divides the incoming scene picture into millions of pixels and measures the colour and brightness of each pixel in binary numbers. A digital image is then generated once the image sensor converts the light to electronic signals.

Cameras are the most widely used perception sensors in ADS. They can capture the wavelengths within a range of $400nm$ to $780nm$ which is the same as that of the human eye. The main advantages of cameras include their ability to sense highly accurate colour information, a relatively higher resolution sensing capability and low cost. It is commonly used to recognise road signs and lane marks in ADS. Nevertheless, the quality of the images captured by cameras can be heavily impaired by various light conditions (e.g. the night light) and adverse weather conditions (rain, fog and snow). As a result, cameras are typically compensated by Lidar sensors for robustness against varying weather conditions [61].

2) Lidar Sensor: While there are many types of 2D and 3D Lidars being used in a variety of applications, including surveying, robotics and autonomous driving, the most common type of Lidars currently seen on ADS is the 3D mechanical rotating Lidars. As shown in Fig. 2, rotating Lidar contains arrays of laser emitters and receivers rotating horizontally at a specific time resolution. The Lasers emit light pulses
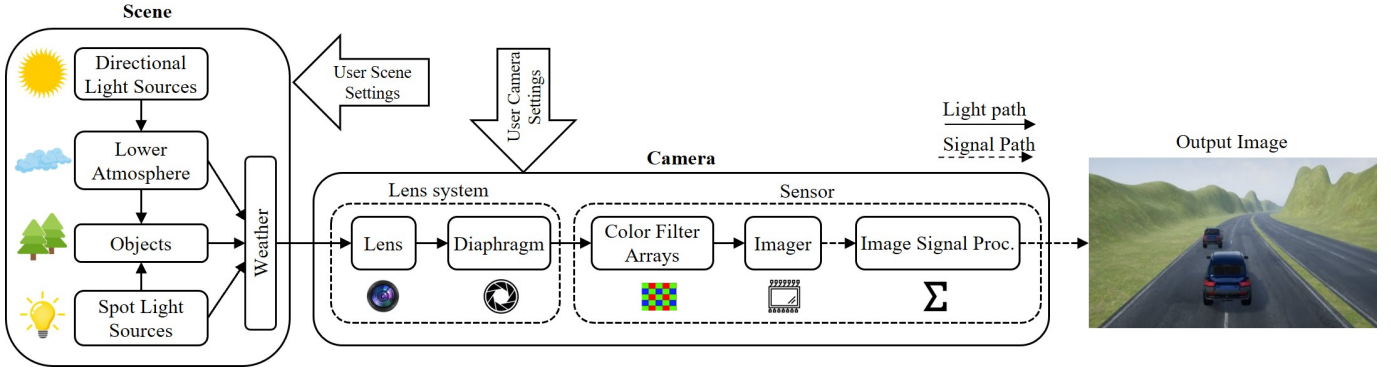
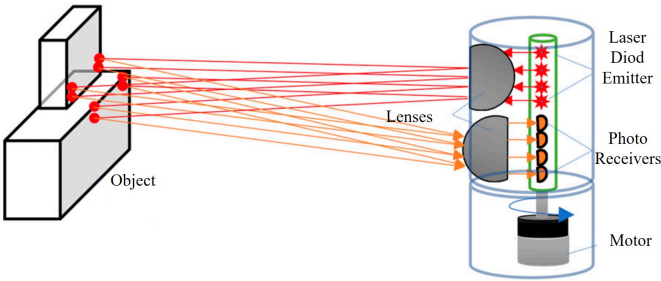Fig. 1: The process of digital image generation. Inspired by a figure in [48].

Fig. 2: Working mechanism of the 3D mechanical rotating Lidar system. The image is sourced from [61].

in Near Infra-Red wavelength, while the receivers filter the incoming signals within that frequency band. The range to a detected target is determined by calculating the time the pulse travels. This information enables the Lidar to generate range data, which serves as the basis for producing an intermediate interface output known as the 3D point cloud.

The wavelength used on automotive Lidars most commonly lies in the range of $850nm$ or $905\ nm$ (with some exceptions of being in $1550nm$), which is within the range that could penetrate the human eye, therefore the laser systems must adapt the Class 1 or Class 1M laser to comply with the safety regulations. This limits the peak power of a single pulse and average power depending on the FOV, pulse burst rate and lens aperture. Consequently, restricting the sensor's range. Currently, typical automotive Lidar sensors can detect objects with a diffuse reflectivity of 10% at a distance of up to approximately 50m, and objects with a diffuse reflectivity of 80% at a distance of 120m [29].

The main advantage of Lidars is their ability to capture high-density 3D data efficiently and accurately. They are also less susceptible to illumination disturbance, such as shadows or bright glares, or reduced lighting conditions, such as night-time, which is critical for autonomous driving. However, the performance of Lidar-based object detection can be significantly affected by various external environmental conditions, including rain, fog, or changes in the reflectance properties of the objects. Furthermore, the data accuracy and density achievable with a particular Lidar sensor are constrained by its hardware specifications. For instance, the performance of a

16-channel Lidar will differ significantly from that of a 128-channel Lidar, and even more so from that of a professional high-resolution 2D Lidar designed specifically for surveying and mapping purposes.

B. Sensor Simulation

Sensor simulation, also known as sensor modelling, employs a set of mathematical functions or computational approximations to map a description of the simulated environment and sensor specification to sensory data that closely resembles what an actual sensor would perceive. Although actual perception sensors such as camera and Lidar provide RGB images and point cloud, several studies have expanded the notion of sensor models to approximate perceived object properties [2], e.g. bounding boxes. Thus, in alignment with the existing literature, we have also considered both raw sensory data and object list as the sensor model's output, as shown in Fig. 3.

Sensor models generally can be categorised into physics-based and learning-based models based on the employed techniques. Physics-based models rely on the detailed calculation of hand-crafted formulas for approximating the physical relationships between the causes and consequences of the sensor disturbances [48]. Physics-based models are popular for their high level of fidelity and, hence, high demand for computational resources. On the other hand, learning-based sensor models, commonly referred to as phenomenological models [60], [31], statistical models [84], or black box methods [9], are utilised to approximate the functionality of individual components or the entire sensor system based on the observed sensory data. The learning-based sensor models are often more efficient and have a lower level of fidelity concerning physics-based models. Due to the huge success of deep learning-based models in discovering complicated patterns and relations [39], learning-based models have gained much popularity in recent years.

III. STATE-OF-THE-ART LEARNING-BASED MODELS

This section provides a thorough review of state-of-the-art learning-based sensor models. We categorise the learning-based sensor models based on their output representation into raw-data-based and object-based models. Raw-data-based models aim to estimate the actual raw sensory data based
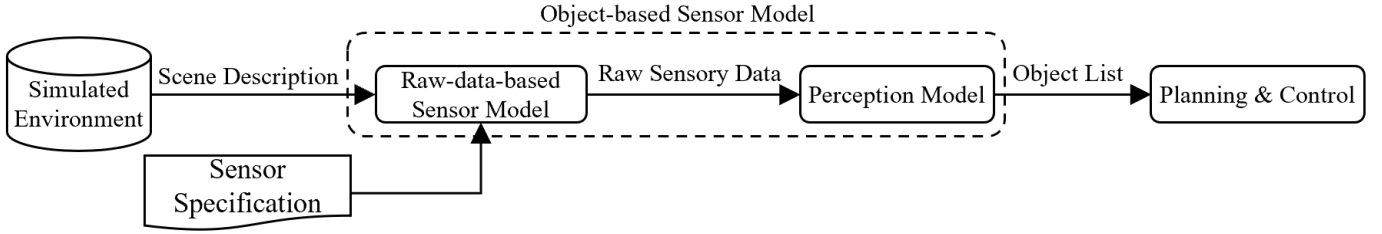
Fig. 3: Overview of perception sensor simulation in ADS.

TABLE I: Summary of learning-based camera and Lidar simulation methods used for ADS applications.

Category	Subcategory	Description	Method
Raw-data-based	Unsupervised (Unconditional)	Two-stage RGB image synthesis using semantic segmentation layout.	[3], [47], [16], [75]
		Modelling Lidar point cloud as range images using GANs without any conditions.	[8],[51],[50]
		Modelling Lidar point cloud as range images using score-based diffusion models without any conditions.	[90]
	Unsupervised (Conditional)	Sim-to-real mapping of driving scenes' images via state-of-the-art unpaired image-to-image translation techniques.	[89], [85], [53], [32],[85],[87],[53]
		Using a deep-learning-based image enhancement network to perform sim-to-real mapping.	[58]
		Adopting CycleGAN for sim-to-real domain transfer of Lidar point clouds represented as BEV images.	[4],[62],[81]
		Using appearance and sparsity GAN modules to perform sim-to-real domain adaptation for Lidar point clouds.	[81]
		Bridging the simulation and real domain gap by learning camera sensor effects.	[10]
	Supervised	Synthesising RGB camera images from the corresponding semantic segmentation layout.	[34], [11], [77], [54], [28]
		Modelling image degradations such as lens effect, weather disturbances, and lighting conditions.	[71], [76], [22], [79],[78]
		Blending images of driving scenes with dynamic objects through the assistance of image enhancement networks.	[12]
		Modelling Lidar intensity and raydrop based on the corresponding range image.	[74], [25], [88], [43]
		Accelerating stereo camera image simulation using neural super-resolution techniques.	[27]
		Modelling images of large street scenes from novel viewpoints using NERFs.	[68] [83]
		Enhancing the realism of primary image renderings obtained by surfel maps.	[82]
		Modelling Lidar point clouds from novel viewpoints using NERFs.	[69]
Object-based	Temporal Error	Modelling object position state over time using auto-regressive or RNN models.	[46],[84], [2]
	Geometric Error	Modelling sensor FOV and occlusion using probabilistic models.	[67],[49]

on a description of the environment (e.g. objects' location, geometry, surface material, etc.) and sensor specification such as the sensor's position and Field Of View (FOV). Raw-data-based models are commonly used to validate perception models, moreover, they are often used to create synthetic datasets for the training of learning-based perception models. On the other hand, object-based models are usually developed by integrating a noise or error element into the ideal object list. The primary objective of object-based models is to test high-level components of ADS, such as control and planning systems. The categorisation of learning-based sensor models is exhibited in Fig. 4. Additionally, a summary of all learning-based sensor models discussed in this paper is provided in Table I.
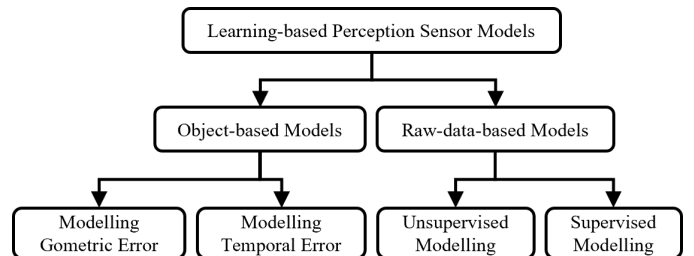

Fig. 4: Categorisation of learning-based perception sensor models.

A. Raw-data-based Methods

Most learning-based sensor models fall under the category of raw-data-based methods. This is attributed to their crucial role in generating sensory data essential for the validation and training of learning-based perception models in ADS. Due to the effectiveness of deep generative models in synthesising high-dimension data [1], the majority of the approaches examined in this section are grounded in these models. The deep generative models leverage the power of extensive sensory datasets and train large neural networks to synthesise sensory data. We categorise the Raw-data-based methods based on their learning approach into unsupervised or supervised methods as it will be explained in the following paragraphs.

1) Unsupervised Modelling Approaches: Unsupervised modelling approaches rely on unsupervised learning techniques to model the raw sensory data. Particularly, the learning process is independent of any predetermined correspondence between synthesised and ground-truth data. Therefore the learning objective focuses on aligning the synthesised data distribution to ground-truth data distribution. We discuss the unsupervised methods within two categories of unconditional and conditional models.

• Unconditional Models: The dataset of real recorded sensory data can be viewed as samples of an underlying data distribution. In this regard, unconditional models attempt to capture this distribution, enabling the generation of a diverse set of random samples for training downstream perception models. Although considering the provided definition of sensor models, there should always be a condition, e.g. scenario description, for a model to operate, this paper discusses unconditional models because they serve as a theoretical foundation for other unsupervised approaches. Considering $Y = \{y \mid y \in \mathbb{R}^N\}$ as a dataset of real recorded N-dimensional sensory data, unconditional models attempt to estimate the data distribution P_Y using the estimator function G. The objective is that the distribution of synthesised data $P_{\hat{Y}}$ be as close as possible to p_Y. After fitting the distribution, a sampler function G can be defined that can generate a sample $\hat{y}$ based on a random vector z as shown in Fig. 5 (a). With the immense success of GANs [23] in generating high-dimensional continuous data, the unconditional approaches mostly leverage the power of this framework in the context of ADS applications. Vanilla GAN framework implicitly learns P_Y by optimising a generator G and a discriminator D in an adversarial manner. The network G attempts to generate fake data that is not distinguishable by D, whereas D targets to discriminate between fake and real data. If the training converges, D should not be able to distinguish between fake and real data, thus G can generate realistic data.

In the area of camera image synthesis, due to the complexity of randomly generating images of driving scenes, unconditional approaches [3], [47], [16], [75] typically divide the creation process into two stages. Initially, a semantic segmentation layout is generated based on a random vector, and subsequently, this layout is conditioned to synthesise the final image. To enable differentiable sampling from the first generator, the Gumbel-softmax [35] trick is used, given that
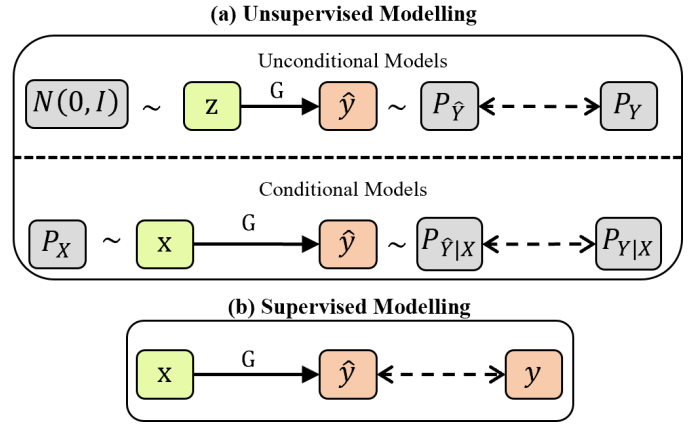

Fig. 5: Overview of unsupervised and supervised modelling approaches in raw-data-based sensor models. The variables $z \sim N(0, I)$, $x \sim P_X$, $y \sim P_Y$, $\hat{y} \sim P_{\hat{Y}(|X)}$ indicate random vector, condition, real sensory data, and synthesised sensory data, respectively.

the semantic segmentation layout is a discrete representation. In the pioneering work, Azadi et al. [3] introduced the Semantic Bottleneck GAN (SB-GAN), which unconditionally creates semantic segmentation layouts and then maps these to images. Following this, Moing et al. [47] proposed using class proportions as a condition for generating semantic segmentation layouts. Their approach requires that the created layouts adhere to the specified class proportions, allowing for improved semantic accuracy and the possibility of editing parts of the layout. Eskandar et al. [16] went further by completely separating the latent variable into super-classes and employing local generators for class-specific feature production. Their research demonstrated that exploring the super-class space results in greater control over the content of the image.

Expanding on the breakthroughs of GANs in creating realistic RGB images, various studies have modified GANs to learn the distribution of Lidar data. Caccia et al. [8] were pioneers in this field, transforming Lidar point clouds into range images and tailoring the Deep Convolutional GAN (DCGAN) [56] for synthesis. Building on this, Nakashima et al. [51] developed the DUSty framework, which integrates ray-drop estimation into the GAN training process. By splitting the creation of Lidar range images into generating clean depth and ray-drop, DUSty achieved more realistic outcomes compared to standard GANs. DUSty2 [50], an advanced version, incorporates Implicit Neural Representation (INR) [65] with GANs, enabling the generation of range images with variable spatial resolutions, thus broadening its use in data restoration and up-sampling.

In the latest work, Zyrianov et al. [90] introduced LIDAR-Gen, a novel GAN-free model, employing score-based diffusion models [66] to better estimate the intrinsic distribution of Lidar point clouds. LIDARGen demonstrated that this score-based technique generates more realistic data by progressively refining the noise in Lidar depth images over time.

• Conditional Models: While unconditional modelling approaches focus on the random generation of diverse data

samples, they lack controllability, a crucial aspect for ADS validation and verification. To address this, conditional models guide the generation process using specific conditions. Since conditions are mostly low-fidelity simulated data in the context of ADS, unsupervised conditional models can be considered as sim-to-real domain mapping functions. Considering $X = \{x \mid x \in \mathbb{R}^M\}$ as a set of simulated data (condition) and $Y = \{y \mid y \in \mathbb{R}^N\}$ as a set of real sensory data, the problem can be formulated as finding the distribution $P_{Y|X}$ using G as the estimator, as shown in Fig. 5(a). With the recent advancements in GANs and their ability to capture data distributions, there has been a surge in the development of GAN-based frameworks for unsupervised image-to-image translation tasks. Among these frameworks, CycleGAN [89] has gained significant popularity and has served as the basis for other techniques in this field. CycleGAN captures the underlying joint distribution of two unpaired image domains by combining GAN and cycle consistency loss. While originally proposed as a general image-to-image translation solution, subsequent works [85], [53] have adopted CycleGAN for sim-to-real domain adaptation, including applications in autonomous driving. In this regard, Isola et al. [32] proposed Cycle-Consistent Adversarial Domain Adaptation (CYCADA) to reduce the gap between the simulated image from GTA5 scenes and real recordings from CityScapes [13] dataset. Following that, Huang et al. [85] proposed MUNIT which was capable of capturing multi-modal distribution. This allows the generation of diverse image samples based on a single simulated input image. Subsequent approaches further proposed different objectives for enforcing consistency instead of cycle consistency. Zhang et al. [87] introduced geometric consistency reducing the solution space specifically in the case of synthesising unnatural textures. More recently, Park et al. [53] utilised contrastive learning to establish consistency between patches of the input and output which has been shown to improve the image quality and reduce the training time.

In the context of Lidar simulation, Saleh et al. [62] and Barrera et al. [4] converted 3D point clouds to Bird-Eye-View (BEV) images and used CycleGAN to transform simulated BEV images from CARLA [14] simulator and real BEV images from KITTI [20] dataset. (An example of this transformation is visualised in Fig. 6) In the subsequent work [81], the 3D point cloud was directly translated between domains utilising two independent GAN modules of appearances and sparsity. The appearance module took the responsibility to transform the 3D shape while the sparsity module simulated the ray drop by making points.

There are also a few studies in the literature that explore alternative approaches to sim-to-real domain adaptation without relying on GANs. One notable study by Ritcher et al [58] thoroughly analysed the limitations of GAN-based methods for sim-to-real image translation, particularly for autonomous driving applications. The authors proposed incorporating strong supervision at multiple perceptual levels and a new sampling strategy for selecting image patches during training. The results demonstrated more realistic and stable image frames mitigating artefacts compared to various baselines, including image translation and style transfer mod-
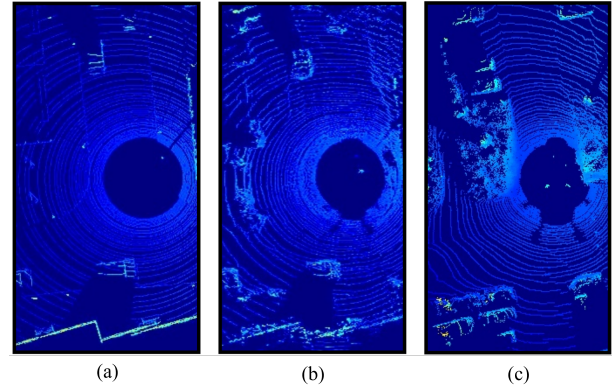

(a) (b) (c)

Fig. 6: An example of unsupervised and conditional Lidar modelling approach. The method [62] performs sim-to-real domain mapping on BEV representation of Lidar point clouds using Cycle-GAN. (a): Simulated point cloud in CARLA, (b): the point cloud synthesised by the Cycle-GAN-based method, and (c): a real point cloud sample from the KITTI dataset. The image is sourced from [62].

els. In another study, Carlson et al. [10] aimed at reducing the domain shift by learning and transferring camera sensor effects. Their proposed transfer network consisted of a series of chained image sensor functions, with learnt parameters, that were trained using style loss. The framework served as a data augmentation method and exhibited improved performance in the Faster R-CNN model [57] on datasets such as KITTI and Cityscapes.

2) Supervised Modelling Approaches: The concept of supervised modelling approaches is derived from supervised learning. In particular, the learning process is directed by the knowledge of the ground-truth real sensory data for each sample of training data. These techniques typically involve learning a particular physical effect or mapping between sensory data channels using real-world data. While the input data can be easily modelled in simulation, generating the corresponding output data often requires significant computational time and resources. Thus, these methods often rely on complicated functions such as neural networks to find the relationships, Considering the input data as $x \in \mathbb{R}^N$, and the corresponding ground-truth as $y \in \mathbb{R}^M$, the supervised modelling approaches attempts to estimate the mapping between the two using G. The objective is to make the predicted output $\hat{y} = G(x)$ as closely aligned as possible with the ground-truth y. The overview of supervised modelling approaches is shown in Fig. 5(b).

In the context of modelling camera images, several methods [34], [11], [77], [54], [28] focus on generating RGB images from the corresponding semantic segmentation layouts. This is because the layouts can be rendered easily and leveraged to generate a wide variety of scene configurations. The methods mostly rely on the conditional GAN [34], [45] framework and incorporate techniques such as multi-scale generation [77], SPatially-Adaptive DEnormalisation (SPADE) [54], and multi-scale SPADE [40] into the generator network.

Other works in this area adopt different strategies. Some

Fig. 7: An example of a supervised modelling approach. The camera image synthesis model, namely SurfelGAN [82], enhances primitive renderings (a.k.a surfel renderings) obtained from a novel view. From top to bottom, rows indicate surfel rendering, surfelGAN output and the corresponding real images. The image is sourced from [82].

techniques use neural networks to render specific image degradation, such as weather disturbances [71], [76], [22], Lens effects [79], and lighting conditions [78] on the input image. The neural networks usually get the clean image as input and synthesise the image containing the effect using adversarial objectives and physics-based approaches. Yang et al. [82] attempted to synthesise realistic camera images based on primitive renderings of driving scenes, namely Surfel maps [55]. The authors proposed an efficient method for reconstructing the scene using a surfel (surface element) map [55] representation of 3D assets. However, as this basic rendering process causes artefacts and inconsistencies, a GAN-based model is leveraged to enhance the quality of the images, called SurfelGAN. The training dataset of SurfelGAN consists of both paired and unpaired image data. An example of the SurfelGAN input and the synthesised output is exhibited in Fig. 7. In a related study by Chen et al. [12], an image composition method was proposed to seamlessly add dynamic objects to image scenes. Their method involved extracting objects from other scenes and reconstructing them using a multi-sensor learning-based approach. The reconstructed objects were added to the image foreground and the realism of the final image was enhanced using a combination of perceptual and adversarial loss. Haghighi et al. [27] introduced a super-resolution network designed to efficiently simulate high-resolution stereo images from their low-resolution counterparts. The method was trained completely on simulated data and has been shown to accelerate the rendering of high-resolution stereo images. In more recent work, Tancik et

al. [68] utilised the concept of the Neural Radiance Field (NERF) [44] to represent large street scenes using neural networks, enabling the synthesis of camera images from a novel viewpoint. To represent the scene efficiently, the authors proposed to split the scene into multiple blocks and train BlockNERF models for each block. The relevant renderings from these blocks are then seamlessly combined to compose the final image from the specified viewpoint.

In the domain of Lidar and 3D point cloud simulation, several works employed U-Net architecture [59], to predict Lidar output modality, e.g. Lidar intensity, using recorded datasets. These neural networks were trained on real data and integrated subsequently as plugins into different simulation frameworks. For instance, Vacek et al. [74] and Wu et al. [80] utilised neural networks to predict Lidar reflectance based on other modalities, e.g. spatial coordinates. Similarly, Guillard et al. [26] and Zhao et al. [88] targeted to estimate Lidar raydrop (i.e. dropout or noise) using learning-based approaches. In a related study by Manivasagam et al. [43], a combination of physics-based and learning-based simulation approaches was utilised to build a Lidar simulator entirely based on recorded data. In this approach, 3D assets were reconstructed by merging Lidar point clouds over time and a ray-tracing algorithm was employed to simulate point clouds at novel virtual positions of ADS. Finally, the simulated points clouds were fed to a deep neural network to synthesise realistic noises. Lately, Tao et al [69] implemented NERF for rendering the Lidar point cloud from a novel viewpoint. Using NERF, they constructed an end-to-end differentiable Lidar simulator enabling the synthesis of Lidar point clouds of high-quality outperforming multi-stage simulation frameworks such as LidarSim [43].

B. Object-based Models

Within the framework of object-based methods, the errors of sensor outputs are mainly related to objects tracked from an ego vehicle. The parameters of an object list usually include object position (both lateral and longitudinal), velocity, acceleration, heading, detection state (detected or undetected), etc. Some parameters (such as object position and velocity) vary as the ego vehicle moves over time, and other parameters (e.g. detection state) are related to geometric occlusions of objects. Thus, we divide the object-based methods in the literature into two categories, namely models of temporal errors and geometric errors respectively.

1) Modelling Temporal Errors: To design a learning-based model regarding temporal sensor errors, the basic idea is to estimate sensor error at time t given the previous sensor error at time $t-1$ [46]. The unseen temporal error signal of sensors can then be sampled from the learned sensor error model. However, it is found that sensor errors are also related to the motion of the ego-vehicle and its environment (e.g. objects around the ego-vehicle), and the sensor errors vary as these conditions change [84]. Thus the object state vector at time t should be considered when learning the sensor error at time t. To model temporal errors, first, sensor errors are calculated as the differences between ground truth sensor data and real sensor data, which can be obtained from public datasets or

self-collected driving data. Then the learning-based sensor model can be generated by fitting a statistical model to the sensor errors or learned through machine learning methods. To be more accurate, the motion of the ego-vehicle and the state of objects around the ego-vehicle should be considered during this process. It is found that non-linear models or complex machine learning models can describe temporal camera sensor errors more accurately compared to linear sensor models, which indicates the complexity of sensor errors. In addition, sensor models using the recurrent neural network can capture long-term temporal sensor errors [2]. We explain details of the methods considering temporal errors in the literature as follows.

Mitra et al. [46] proposed a model for the bounding box offset of the object detection by the camera sensor on the ADS. The bounding box offset in [46] referred to the difference between the ground truth coordinates and the sensor-measured coordinates of the top-left and bottom-right corners of a bounding box (the object detection result). They used two subsets from the KITTI object tracking evaluation [21] in which the driving data was collected in highways and urban areas. The Faster R-CNN [57] was selected in [46] as the object detection method for the camera sensor. To model the time series of the bounding box offset, the authors adopted a linear auto-regressive moving average model [6], [73] and a nonlinear auto-regressive model respectively, which can predict future values of a given time series. A Bayesian information criterion [19] was adopted as the model selection method to choose the best-fit model. Experimental results in [46] showed that the non-linear auto-regressive model had better performance in fitting the bounding box offset series compared to the linear auto-regressive model.

Zec et al. [84] developed a model based on the observation that errors vary as the motion of the ego-vehicle and its environment change. The authors proposed a statistical model that uses the auto-regressive input-output hidden Markov model (AIOHMM) technique to predict time-variant sensor errors. The model specifically focused on the error in the longitudinal position of the object over time. However, it was claimed that other state parameters of the object can be estimated using the same method. Sensory data in real-world traffic conditions (country roads and highways in Europe) was collected for learning, and an off-the-shelf sensor setup from Volvo Car Corporation was used. A Velodyne Lidar HDL-64E was used in the vehicle working as the reference of object parameters. Thus, the considered sensor error referred to the differences between fused sensor data and the ground truth data generated by the Lidar sensor.

Arnelid et al. [2] extended the generative sensor error model of the previous model [84] by proposing an improved deep learning model, recurrent conditional generative adversarial networks (RC-GAN). The model combined the recurrent neural network (RNN) and the generative adversarial network to generate the sensor error showing long-term temporal correlations. This model was based on the networks described in work by Esteban et al. [17], in which the generator and discriminator in the original GAN [23] were replaced by RNNs with long short-term memory units. Arnelid et al. [2] adapted
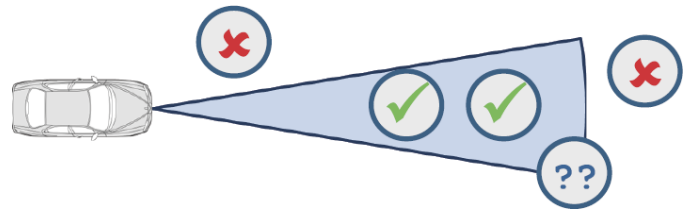

Fig. 8: Modelling geometrical errors in object-based camera model. The model decides which objects are within the FOV of the specified camera sensor. The partly overlapping objects required special consideration. The image is sourced from [67].

this model to sensor error modelling. They improved this model by isolating the noise to its own RNN and adding a skip connection to the generator and discriminator. The study mainly focused on the sensor error in estimating the longitudinal position, lateral position and velocity of the tracked object. The authors adopted a sensor setup known as AIOHMM [84], thus the sensor error was generated by a series defined by the differences between the fusion sensor output and ground truth Lidar sensor output over time. Real driving data on European highways and trunk roads were collected to learn the RC-GAN model. Experimental results on the validation dataset showed significant improvement in temporal sensor error modelling compared with AIOHMM and the original RC-GAN [17].

2) Modelling Geometric Errors: The geometric errors of sensors mainly refer to the detection states of objects tracked by an ego-vehicle, including the detected, undetected, newly detected, etc. When modelling the geometric errors of camera sensors, researchers usually need to consider the degree of the object occlusion to determine the detection state of an object, by defining the detection range of the sensor on ADS first, and then checking whether the object is geometrically within the detection range of the sensor and whether the object is blocked by other obstacles. Stolz et al. [67] proposed a fast generic sensor model for virtual testing and validation of highly autonomous driving functions. The generic sensor model used a ground truth object list as input and processed it based on the visibility of the object by labelling the status of the object (not detected, detected, newly detected) as shown in Fig. 8. The authors focused on two aspects of sensor simulation: object detection and the visibility of the detected object. A radial basis function [7] was used in this model to define the detection range and determine whether the object was geometrically within the detection range of the camera sensor. The ratio of the unblocked to the blocked view angle of the object from the vehicle's point of view was used to determine whether an object was occluded by an obstacle. This flexible method allowed the sensor model to determine the detection of an object with arbitrary geometry.

Muckenhuber et al. [49] introduced an approach to alter incoming object lists based on various sensor specifications. These specifications include the field-of-view (FOV), class definitions, and probabilities of false detections. The authors represent FOV as a two-dimensional polygon, allowing the exclusion of objects outside the FOV and the recognition
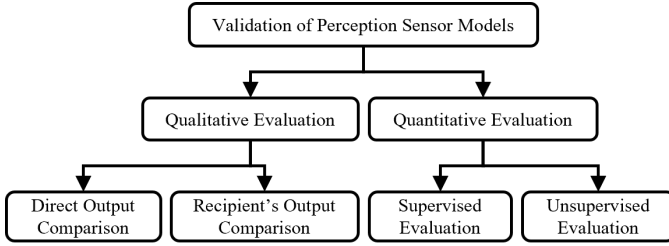
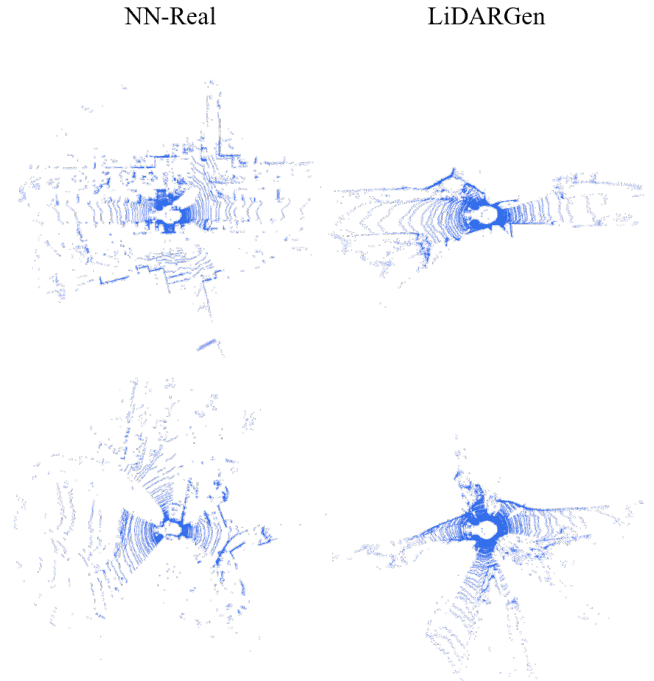Fig. 9: Categorising validation approaches of perception sensor models.

Fig. 10: Qualitative validation of Lidar model by direct comparison. The synthesised point cloud of LidarGen [90] is compared to the nearest neighbour real point cloud (NN-Real). The image is sourced from [90].

of objects within it. Additionally, they incorporated user-defined lookup tables to map ground-truth class definitions onto sensor-specific definitions. False negative and false positive detections were simulated on the remaining objects using probabilistic functions, the parameters of which were derived from real sensory data. Probabilistic relationships control the inclusion of false negative and false positive detections, adding a layer of realism to the simulated sensor outputs.

IV. VALIDATION OF PERCEPTION SENSOR MODELS

Similar to any other modelling approach, it is crucial to thoroughly evaluate the performance of sensor models concerning their intended role within the system [52]. In the validation of perception sensor models for ADS, two general methodologies, namely qualitative and quantitative evaluation, are commonly employed. Qualitative evaluation involves visualising either the output of the sensor model itself or the output of a recipient component, such as a perception model. On the other hand, quantitative evaluation entails assessing the model based on either supervised metrics, when reference data is available, or unsupervised metrics, when reference data is not accessible. The categorisation of validation methods is depicted in Fig. 9. In the subsections below, we will explore existing examples of both qualitative and quantitative evaluations in the literature of camera and Lidar models for ADS.

A. Qualitative Evaluation

Qualitative evaluation is the most common approach for validating perception sensor models. This process involves visualising the output of the sensor model and comparing it to state-of-the-art methods and real data. Moreover, some studies emphasise visualising the output of a perception model, such as a semantic segmentation network. A more detailed exploration of these two qualitative evaluation approaches is provided in the subsequent paragraphs.

1) Direct Output Visualisation: Nearly all the discussed camera and Lidar models visualise their synthesised outputs and compare them with both real data and state-of-the-art methods. The input data for sensor models is also visualised (except in unconditional approaches), to understand the information from which the model learns. For example, in the sim-to-real mapping network introduced by [58], various simulated buffers such as normal, depth, and albedo, are processed and then visualised during the evaluation phase. For comparison

with real sensory data, the model's output is either compared to ground-truth data in cases of supervised methods, or with nearest neighbour samples from the training dataset regarding unsupervised approaches (see Fig. 10). In instances like the LidarSim [43] framework, the entire scene is reconstructed using real data, providing corresponding ground-truth for each Lidar viewpoint. Conversely, Dusty [51] generates data randomly, and the nearest neighbour samples from real data are used for comparison. Regarding data representation, camera models often visualise synthesised RGB images, whereas Lidar models visualise BEV images, range images or 3D point clouds based on the employed data representation.

Additionally, the learned models are sometimes used in applications such as data restoration, with the results being visualised. For example, Dusty2 [50] model was used to reconstruct real range images or restore distorted images. The high-quality restored or reconstructed images demonstrate the model's ability to cover data distribution effectively.

2) Recipient's Output Comparison: As perception sensors are not standalone systems in ADS, it is essential to consider their integration with downstream components that receive sensory data. Considering a learning-based perception model as the recipient component, several studies [32], [74], [25], [43] have visualised the predicted annotations of the models. This approach allows for evaluating the performance of the models that have been trained on synthesised data using real test data. The closer the output of the sensor model resembles the real-world data, the higher the accuracy of the perception model in detecting and interpreting its input. Fig.
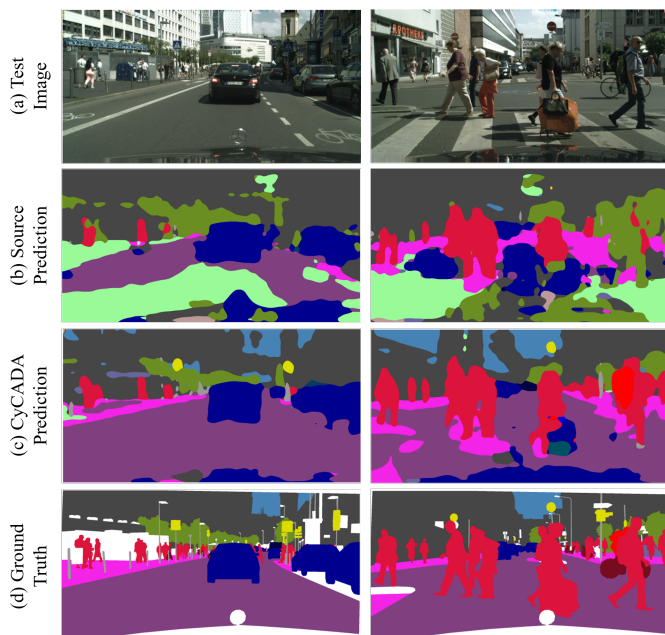
Fig. 11: Qualitative validation of camera model by comparing the output of a downstream task, e.g. semantic segmentation network. The semantic segmentation network is trained with two different image sources: (1) synthetic images of the GTA-V dataset, and (2) the modelled ones by CyCADA. The test images (a) are fed to these networks and the prediction is depicted in (b) and (c), respectively. The last row (d) shows the ground-truth layout. The image is sourced from [32].

11 demonstrates an example of evaluating a sensor model (CyCADA [32]) through predictions of a semantic segmentation network, FCN [64]. As shown, the FCN model is much more accurate when trained on CyCADA's synthesised images than on the source images. This demonstrates the effectiveness of CyCADA in improving the realism of GTA-V simulated images.

B. Quantitative Evaluation

Quantitative evaluation of sensor models entails establishing a mathematical metric to measure the model's performance against the expected output. We categorise these quantitative evaluation methods into supervised and unsupervised groups. Supervised evaluation techniques require paired model input and ground-truth output for the assessment, while unsupervised evaluation techniques do not enforce such necessity. We will explain the quantitative evaluation techniques in more detail in the following paragraphs.

1) Supervised Evaluation: To quantitatively validate a sensor model in a supervised manner, it is necessary to establish correspondence between the synthesised sensory data and the real-world data. The supervised evaluation methods are often utilised in supervised modelling approaches where the models are trained with a pair of input-output data, thus enabling comparison with ground-truth. For instance, in the cases where semantic summation layout is transformed into RGB images or Lidar intensity is predicted using the spatial coordinates, the

TABLE II: Summary of quantitative evaluation metrics.

Category	Description	Metric
Supervised	pixel-level error measurement	RMSE, MAE, PSNR
	perceptual similarity	SSIM, LPIPS [86]
	3D point cloud distance	CD, EMD [18]
Unsupervised	distribution distance (images)	FID [30], KID [5], sKVD [58], SWD [38]
	distribution distance (point clouds)	JSD [18], MMD [18]
	distribution diversity	COV [18], 1-NNA [18]
	perception model's performance	IOU, mAP, pixAcc, classAcc

ground-truth RGB or intensity image in the test set is used for the supervised evaluation. Similarly, other frameworks such as SurfelGAN [82] and LidarSim [43] reconstruct the 3D scene using real sensory data frames, thus providing access to the expected models' output at specific viewpoints of the sensor.

Supervised evaluation metrics commonly focus on calculating the average per-pixel error in image-based sensory data representations. These metrics include Root Mean Squared Error (RMSE, i.e. L2 distance error), Mean Absolute Error (MAE, L1 distance error), thresholded accuracy (ratio of pixels with the error less than a certain threshold), and PSNR. For calculating the distance of the Lidar point cloud in 3D representation, Chamfer Distance (CD) and Earth Mover's Distance (EMD) [18] are frequently utilised. Additionally, other supervised metrics such as SSIM and LPIPS [86] are used, relying on structural and feature similarity rather than solely on pixel-level error.

2) Unsupervised Evaluation: Building an environment model that accurately reflects complex real-world scenarios is a challenging task. Therefore, there is often no direct correspondence between real and synthesised sensory data, thus unsupervised evaluation methods are commonly employed. These methods typically rely on constructing two sets of synthesised and real data, considering them as distributions, and employing metrics to calculate the distance between these distributions. Frechet Inception Distance (FID) [30], Kernel Inception Distance (KID) [5], and Sliced Wasserstein Distance (SWD) [38] are common metrics used to measure this distance for the sensory data represented as images. In the work by Ritcher et al. [58], the authors proposed semantically aligned Kernel VGG distance (sKVD) that addresses the bias toward semantic similarity of the scenes, a limitation often found in FID/KID. Concerning finding the distance between distributions of two Lidar 3D point clouds, Jensen-Shannon Divergence (JSD) and Minimum Matching distance (MMD) have also been employed [51]. In assessing the performance of unconditional modelling approaches, metrics such as Coverage (COV) and 1-Nearest Neighbour Accuracy (1-NNA) have also been used [51] to measure the diversity of generated samples.

Some studies have also incorporated human perceptual studies [11] to measure the realism of the synthesised RGB images. This evaluation involves visualising the paired synthesised and real images to the human users and reporting the percentage of times when users preferred the synthesised image. The

studies commonly used the Amazon Mechanical Turk (AMT) platform for conducting evaluations.

The most widely used unsupervised evaluation approach found in the literature involves assessing the performance of a downstream perception model. This process starts by conducting a set of synthesised sensory data to train the perception model. After training with the synthesised dataset, the perception model is then validated on a real sensory dataset. The performance of the perception model is compared to its performance when initially trained on real data. The principle of this approach is that the closer the perception model's performance to its performance on real data, the more realistic the synthesised data is perceived by the model. Typically, the perception models used in these evaluations are state-of-the-art object detection or semantic segmentation models. Key performance metrics for these models include Intersection Over Union (IOU), average Precision (AP), average pixel accuracy (pixAcc), and average class accuracy (classAcc). The summary of the quantitative evaluation metrics is provided in Table II.

V. Conclusion and Research Gaps

In this review, we discussed the state-of-the-art learning-based camera and Lidar simulation techniques for the development and validation of ADS. Our review covered both raw-data-based and object-based sensor models in the literature from the perspective of unsupervised and supervised modelling approaches. Additionally, we highlighted the importance of sensor model validation, exploring various approaches employed in this domain.

Although learning-based sensor models, particularly those based on deep learning, have shown promising outcomes in recent years, concerns exist surrounding their explainability and reliability specifically in challenging scenarios. Moreover, these models have mostly been applied to offline applications such as enhancing the downstream perception algorithms, leaving their adequacy for online applications, e.g. HIL testing, less investigated. Deep learning-based models also pose trustworthiness concerns [33] as they encounter difficulties while generalising to scenarios beyond the training data distribution. Furthermore, the lack of standardised mechanisms or benchmarks to assess the fidelity of sensor models in representing real-world sensor behaviour underlines critical gaps in current validation techniques. We hope that this review opens the door for further research aimed at improving the reliability, efficiency and fidelity of learning-based sensor models in the context of ADS applications.

Acknowledgment

References

[1] A. Alotaibi. Deep generative adversarial networks for image-to-image translation: A review. Symmetry, 12(10):1705, 2020.

[2] H. Arnelid, E. L. Zec, and N. Mohammadiha. Recurrent conditional generative adversarial networks for autonomous driving sensor modelling. In 2019 IEEE Intelligent Transportation Systems Conference (ITSC), pages 1613–1618, Oct 2019.

[3] S. Azadi, M. T. Tschannen, E. Tzeng, S. Gelly, T. Darrell, and M. Lučić. Semantic bottleneck scene generation. Technical report, 2019.

[4] A. Barrera, J. Beltrán, C. Guindel, J. A. Iglesias, and F. García. Cycle and semantic consistent adversarial domain adaptation for reducing simulation-to-real domain shift in lidar bird's eye view. In 2021 IEEE International Intelligent Transportation Systems Conference (ITSC), page 3081–3086. IEEE Press, 2021.

[5] M. Bińkowski, D. J. Sutherland, M. Arbel, and A. Gretton. Demystifying MMD GANs. In International Conference on Learning Representations, 2018.

[6] G. E. P. Box, G. M. Jenkins, G. C. Reinsel, and G. M. Ljung. Time Series Analysis: Forecasting and Control. John Wiley and Sons Inc., 5th edition, 2015.

[7] M. Buhmann. Radial basis functions: Theory and implementations. Radial Basis Functions, 12, 01 2003.

[8] L. Caccia, H. van Hoof, A. C. Courville, and J. Pineau. Deep generative modeling of lidar data. 2019 IEEE/RSJ International Conference on Intelligent Robots and Systems (IROS), pages 5034–5040, 2018.

[9] P. Cao, W. Wachenfeld, and H. Winner. Perception sensor modeling for virtual validation of automated driving. it - Information Technology, 57, 01 2015.

[10] A. Carlson, K. A. Skinner, R. Vasudevan, and M. Johnson-Roberson. Sensor transfer: Learning optimal sensor effect image augmentation for sim-to-real domain adaptation. IEEE Robotics and Automation Letters, 4:2431–2438, 2018.

[11] Q. Chen and V. Koltun. Photographic image synthesis with cascaded refinement networks. 2017 IEEE International Conference on Computer Vision (ICCV), pages 1520–1529, 2017.

[12] Y. Chen, F. Rong, S. Duggal, S. Wang, X. Yan, S. Manivasagam, S. Xue, E. Yumer, and R. Urtasun. Geosim: Realistic video simulation via geometry-aware composition for self-driving. 2021 IEEE/CVF Conference on Computer Vision and Pattern Recognition (CVPR), pages 7226–7236, 2021.

[13] M. Cordts, M. Omran, S. Ramos, T. Rehfeld, M. Enzweiler, R. Benenson, U. Franke, S. Roth, and B. Schiele. The cityscapes dataset for semantic urban scene understanding. In Proc. of the IEEE Conference on Computer Vision and Pattern Recognition (CVPR), 2016.

[14] A. Dosovitskiy, G. Ros, F. Codevilla, A. M. López, and V. Koltun. Carla: An open urban driving simulator. ArXiv, abs/1711.03938, 2017.

[15] A. Elmquist and D. Negrut. Modeling cameras for autonomous vehicle and robot simulation: An overview. IEEE Sensors Journal, 21(22):25547–25560, 2021.

[16] G. Eskandar, Y. Farag, T. Yenamandra, D. Cremers, K. Guirguis, and B. Yang. Urban-stylegan: Learning to generate and manipulate images of urban scenes, 2023.

[17] C. Esteban, S. Hyland, and G. Rätsch. Real-valued (medical) time series generation with recurrent conditional gans. 06 2017.

[18] H. Fan, H. Su, and L. J. Guibas. A point set generation network for 3d object reconstruction from a single image. 2017 IEEE Conference on Computer Vision and Pattern Recognition (CVPR), pages 2463–2471, 2016.

[19] D. Findley. Counterexamples to parsimony and bic. Annals of the Institute of Statistical Mathematics, 43:505–514, 02 1991.

[20] A. Geiger, P. Lenz, C. Stiller, and R. Urtasun. Vision meets robotics: The kitti dataset. International Journal of Robotics Research (IJRR), 2013.

[21] A. Geiger, P. Lenz, and R. Urtasun. Are we ready for autonomous driving? the kitti vision benchmark suite. pages 3354–3361, 05 2012.

[22] R. Gong, D. Dai, Y. Chen, W. Li, and L. V. Gool. Analogical image translation for fog generation. arXiv, 6 2020.

[23] I. Goodfellow, J. Pouget-Abadie, M. Mirza, B. Xu, D. Warde-Farley, S. Ozair, A. Courville, and Y. Bengio. Generative adversarial nets. In Z. Ghahramani, M. Welling, C. Cortes, N. Lawrence, and K. Weinberger, editors, Advances in Neural Information Processing Systems, volume 27. Curran Associates, Inc., 2014.

[24] S. M. Grigorescu, B. Trasnea, T. T. Cocias, and G. Macesanu. A survey of deep learning techniques for autonomous driving. Journal of Field Robotics, 37:362 – 386, 2019.

[25] B. Guillard, S. Vemprala, J. K. Gupta, O. Miksik, V. Vineet, P. Fua, and A. Kapoor. Learning to simulate realistic lidars. pages 8173–8180, 9 2022.

[26] B. Guillard, S. Vemprala, J. K. Gupta, O. Miksik, V. Vineet, P. Fua, and A. Kapoor. Learning to simulate realistic lidars, 2022.

[27] H. Haghighi, M. Dianati, V. Donzella, and K. Debattista. Accelerating stereo image simulation for automotive applications using neural stereo super resolution. IEEE Transactions on Intelligent Transportation Systems, 24(11):12627–12636, 2023.

[28] M. Hariat, O. Laurent, R. Kazmierczak, S. Zhang, A. Bursuc, A. Yao, and G. Franchi. Learning to generate training datasets for robust semantic segmentation, 2023.

[29] J. Hecht. Lidar for self-driving cars. Optics and Photonics News, 29(1):26–33, 2018.

[30] M. Heusel, H. Ramsauer, T. Unterthiner, B. Nessler, and S. Hochreiter. Gans trained by a two time-scale update rule converge to a local nash equilibrium. In Neural Information Processing Systems, 2017.

[31] N. Hirsenkorn, T. Hanke, A. Rauch, B. Dehlink, R. Rasshofer, and E. Biebl. A non-parametric approach for modeling sensor behavior. In 2015 16th International Radar Symposium (IRS), pages 131–136. IEEE, 2015.

[32] J. Hoffman, E. Tzeng, T. Park, J.-Y. Zhu, P. Isola, K. Saenko, A. Efros, and T. Darrell. CyCADA: Cycle-consistent adversarial domain adaptation. In J. Dy and A. Krause, editors, Proceedings of the 35th International Conference on Machine Learning, volume 80 of Proceedings of Machine Learning Research, pages 1989–1998. PMLR, 10–15 Jul 2018.

[33] X. Huang, D. Kroening, W. Ruan, J. Sharp, Y. Sun, E. Thamo, M. Wu, and X. Yi. A survey of safety and trustworthiness of deep neural networks: Verification, testing, adversarial attack and defence, and interpretability. Comput. Sci. Rev., 37:100270, 2018.

[34] P. Isola, J.-Y. Zhu, T. Zhou, and A. A. Efros. Image-to-image translation with conditional adversarial networks. 2017 IEEE Conference on Computer Vision and Pattern Recognition (CVPR), pages 5967–5976, 2016.

[35] E. Jang, S. Gu, and B. Poole. Categorical reparameterization with gumbel-softmax. CoRR, abs/1611.01144, 2016.

[36] N. Kalra and S. Paddock. Driving to safety: How many miles of driving would it take to demonstrate autonomous vehicle reliability? Transportation Research Part A: Policy and Practice, 94:182–193, 12 2016.

[37] Y. Kang, H. Yin, and C. Berger. Test your self-driving algorithm: An overview of publicly available driving datasets and virtual testing environments. IEEE Transactions on Intelligent Vehicles, 4(2):171–185, 2019.

[38] T. Karras, T. Aila, S. Laine, and J. Lehtinen. Progressive growing of gans for improved quality, stability, and variation. ArXiv, abs/1710.10196, 2017.

[39] Y. LeCun, Y. Bengio, and G. Hinton. Deep learning. nature, 521(7553):436, 2015.

[40] S. Li, M.-M. Cheng, and J. Gall. Dual pyramid generative adversarial networks for semantic image synthesis. In British Machine Vision Conference, 2022.

[41] W. Liu, Q. Dong, P. Wang, G. Yang, L. Meng, Y. Song, Y. Shi, and Y. Xue. A survey on autonomous driving datasets. In 2021 8th International Conference on Dependable Systems and Their Applications (DSA), pages 399–407, 2021.

[42] Z. Liu, S. Minghao, J. Zhang, S. Liu, H. Blasinski, T. Lian, and B. Wandell. A system for generating complex physically accurate sensor images for automotive applications. Electronic Imaging, 2019:53–1, 01 2019.

[43] S. Manivasagam, S. Wang, K. Wong, W. Zeng, M. Sazanovich, S. Tan, B. Yang, W.-C. Ma, and R. Urtasun. Lidarsim: Realistic lidar simulation by leveraging the real world. In Proceedings of the IEEE/CVF Conference on Computer Vision and Pattern Recognition, pages 11167–11176, 2020.

[44] B. Mildenhall, P. P. Srinivasan, M. Tancik, J. T. Barron, R. Ramamoorthi, and R. Ng. Nerf: Representing scenes as neural radiance fields for view synthesis. In ECCV, 2020.

[45] M. Mirza and S. Osindero. Conditional generative adversarial nets. ArXiv, abs/1411.1784, 2014.

[46] P. Mitra, A. Choudhury, V. R. Aparow, G. Kulandaivelu, and J. Dauwels. Towards modeling of perception errors in autonomous vehicles. In 2018 21st International Conference on Intelligent Transportation Systems (ITSC), pages 3024–3029, 2018.

[47] G. L. Moing, T. Vu, H. Jain, P. Perez, and M. Cord. Semantic palette: Guiding scene generation with class proportions. In 2021 IEEE/CVF Conference on Computer Vision and Pattern Recognition (CVPR), pages 9338–9346, Los Alamitos, CA, USA, jun 2021. IEEE Computer Society.

[48] R. Molenaar, A. van Bilsen, R. van der Made, and R. de Vries. Full spectrum camera simulation for reliable virtual development and validation of adas and automated driving applications. In 2015 IEEE Intelligent Vehicles Symposium (IV), pages 47–52, June 2015.

[49] S. Muckenhuber, H. Holzer, J. Rübsam, and G. Stettinger. Object-based sensor model for virtual testing of adas/ad functions. 2019 IEEE International Conference on Connected Vehicles and Expo (ICCVE), pages 1–6, 2019.

[50] K. Nakashima, Y. Iwashita, and R. Kurazume. Generative range imaging for learning scene priors of 3d lidar data, 2022.

[51] K. Nakashima and R. Kurazume. Learning to drop points for lidar scan synthesis. 2021 IEEE/RSJ International Conference on Intelligent Robots and Systems (IROS), pages 222–229, 2021.

[52] W. L. Oberkampf and T. G. Trucano. Verification and validation benchmarks. Nuclear Engineering and Design, 238(3):716–743, 2008. Benchmarking of CFD Codes for Application to Nuclear Reactor Safety.

[53] T. Park, A. A. Efros, R. Zhang, and J.-Y. Zhu. Contrastive learning for unpaired image-to-image translation. In Computer Vision – ECCV 2020: 16th European Conference, Glasgow, UK, August 23–28, 2020, Proceedings, Part IX, page 319–345, Berlin, Heidelberg, 2020. Springer-Verlag.

[54] T. Park, M.-Y. Liu, T.-C. Wang, and J.-Y. Zhu. Semantic image synthesis with spatially-adaptive normalization. In 2019 IEEE/CVF Conference on Computer Vision and Pattern Recognition (CVPR), pages 2332–2341, 2019.

[55] H. Pfister, M. Zwicker, J. van Baar, and M. Gross. Surfels: Surface elements as rendering primitives. In Proceedings of the 27th Annual Conference on Computer Graphics and Interactive Techniques, SIG-GRAPH '00, page 335–342, USA, 2000. ACM Press/Addison-Wesley Publishing Co.

[56] A. Radford, L. Metz, and S. Chintala. Unsupervised representation learning with deep convolutional generative adversarial networks. CoRR, abs/1511.06434, 2015.

[57] S. Ren, K. He, R. Girshick, and J. Sun. Faster r-cnn: Towards real-time object detection with region proposal networks. In C. Cortes, N. D. Lawrence, D. D. Lee, M. Sugiyama, and R. Garnett, editors, Advances in Neural Information Processing Systems 28, pages 91–99. Curran Associates, Inc., 2015.

[58] S. R. Richter, H. Alhaija, and V. Koltun. Enhancing photorealism enhancement. IEEE Transactions on Pattern Analysis & Machine Intelligence, 45(02):1700–1715, feb 2023.

[59] O. Ronneberger, P. Fischer, and T. Brox. U-net: Convolutional networks for biomedical image segmentation. In N. Navab, J. Hornegger, W. M. Wells, and A. F. Frangi, editors, Medical Image Computing and Computer-Assisted Intervention – MICCAI 2015, pages 234–241, Cham, 2015. Springer International Publishing.

[60] P. Rosenberger, M. Holder, M. Zirulnik, and H. Winner. Analysis of real world sensor behavior for rising fidelity of physically based lidar sensor models. In 2018 IEEE Intelligent Vehicles Symposium (IV), pages 611–616. IEEE, 2018.

[61] F. Rosique, P. Navarro Lorente, C. Fernandez, and A. Padilla. A systematic review of perception system and simulators for autonomous vehicles research. Sensors, 19:648, 02 2019.

[62] K. Saleh, A. Abobakr, M. Attia, J. Iskander, D. Nahavandi, M. Hossny, and S. Nahvandi. Domain adaptation for vehicle detection from bird's eye view lidar point cloud data. In 2019 IEEE/CVF International Conference on Computer Vision Workshop (ICCVW), pages 3235–3242, 2019.

[63] Schlager, Muckenhuber, SchmidtSchlager, and Holzer. State-of-the-art sensor models for virtual testing of advanced driver assistance systems/autonomous driving functions. SAE Intl J, 2020.

[64] E. Shelhamer, J. Long, and T. Darrell. Fully convolutional networks for semantic segmentation. IEEE Transactions on Pattern Analysis and Machine Intelligence, 39(4):640–651, 2017.

[65] V. Sitzmann, J. N. Martel, A. W. Bergman, D. B. Lindell, and G. Wetzstein. Implicit neural representations with periodic activation functions. In Proc. NeurIPS, 2020.

[66] Y. Song and S. Ermon. Generative Modeling by Estimating Gradients of the Data Distribution. Curran Associates Inc., Red Hook, NY, USA, 2019.

[67] M. Stolz and G. Nestlinger. Fast generic sensor models for testing highly automated vehicles in simulation. e & i Elektrotechnik und Informationstechnik, 135, 07 2018.

[68] M. Tancik, V. Casser, X. Yan, S. Pradhan, B. P. Mildenhall, P. Srinivasan, J. T. Barron, and H. Kretzschmar. Block-nerf: Scalable large scene neural view synthesis. In 2022 IEEE/CVF Conference on Computer Vision and Pattern Recognition (CVPR), pages 8238–8248, Los Alamitos, CA, USA, jun 2022. IEEE Computer Society.

[69] T. Tao, L. Gao, G. Wang, Y. Lao, P. Chen, H. Zhao, D. Hao, X. Liang, M. Salzmann, and K. Yu. Lidar-nerf: Novel lidar view synthesis via neural radiance fields, 2023.

[70] Tesla. Tesla in fatal california crash was on autopilot. Available at https://www.bbc.co.uk/news/world-us-canada-43604440 (accessed: 14.07.2020).

[71] M. Tremblay, S. S. Halder, R. de Charette, and J. F. Lalonde. Rain rendering for evaluating and improving robustness to bad weather. International Journal of Computer Vision, pages 1–20, 9 2020.

[72] Uber. Uber in fatal crash had safety flaws say us investigators. Available at https://www.bbc.co.uk/news/business-50312340 (accessed: 14.07.2020).

[73] G. Udny Yule. On a Method of Investigating Periodicities in Disturbed Series, with Special Reference to Wolfer's Sunspot Numbers. Philosophical Transactions of the Royal Society of London Series A, 226:267–298, Jan. 1927.

[74] P. Vacek, O. Jašek, K. Zimmermann, and T. Svoboda. Learning to predict lidar intensities. IEEE Transactions on Intelligent Transportation Systems, 23(4):3556–3564, 2022.

[75] A. Volokitin, E. Konukoglu, and L. Van Gool. Decomposing image generation into layout prediction and conditional synthesis. In 2020 IEEE/CVF Conference on Computer Vision and Pattern Recognition Workshops (CVPRW), pages 1530–1538, 2020.

[76] H. Wang, Z. Yue, Q. Xie, Q. Zhao, Y. Zheng, and D. Meng. From rain generation to rain removal. arXiv, 8 2020.

[77] T.-C. Wang, M.-Y. Liu, J.-Y. Zhu, A. Tao, J. Kautz, and B. Catanzaro. High-resolution image synthesis and semantic manipulation with conditional gans. 2018 IEEE/CVF Conference on Computer Vision and Pattern Recognition, pages 8798–8807, 2017.

[78] Z. Wang, W. Chen, D. Acuna, J. Kautz, and S. Fidler. Neural light field estimation for street scenes with differentiable virtual object insertion. In Computer Vision – ECCV 2022: 17th European Conference, Tel Aviv, Israel, October 23–27, 2022, Proceedings, Part II, page 380–397, Berlin, Heidelberg, 2022. Springer-Verlag.

[79] C. Wittpahl, H. B. Zakour, M. Lehmann, and A. Braun. Realistic image degradation with measured psf, 2018.

[80] B. Wu, X. Zhou, S. Zhao, X. Yue, and K. Keutzer. Squeezesegv2: Improved model structure and unsupervised domain adaptation for road-object segmentation from a lidar point cloud. Proceedings - IEEE International Conference on Robotics and Automation, 2019-May:4376–4382, 9 2018.

[81] A. Xiao, J. Huang, D. Guan, F. Zhan, and S. Lu. Synlidar: Learning from synthetic lidar sequential point cloud for semantic segmentation. arXiv preprint arXiv:2107.05399, 2021.

[82] Z. Yang, Y. Chai, D. Anguelov, Y. Zhou, P. Sun, D. Erhan, S. Rafferty, and H. Kretzschmar. Surfelgan: Synthesizing realistic sensor data for autonomous driving. In Proceedings of the IEEE/CVF Conference on Computer Vision and Pattern Recognition (CVPR), June 2020.

[83] Z. Yang, Y. Chen, J. Wang, S. Manivasagam, W.-C. Ma, A. J. Yang, and R. Urtasun. Unisim: A neural closed-loop sensor simulator. In CVPR, 2023.

[84] E. L. Zec, N. Mohammadiha, and A. Schliep. Statistical sensor modelling for autonomous driving using autoregressive input-output hmms. In 2018 21st International Conference on Intelligent Transportation Systems (ITSC), pages 1331–1336, Nov 2018.

[85] C. Zhang, W. Xi, X. Liu, G. Bai, J. Sun, and F. Yu. Unsupervised multimodal image-to-image translation: Generate what you want. In 2022 International Joint Conference on Neural Networks (IJCNN), pages 1–8, 2022.

[86] R. Zhang, P. Isola, A. A. Efros, E. Shechtman, and O. Wang. The unreasonable effectiveness of deep features as a perceptual metric. 2018 IEEE/CVF Conference on Computer Vision and Pattern Recognition, pages 586–595, 2018.

[87] Y. Zhang, S. Wang, B. Chen, and J. Cao. Gcgan: Generative adversarial nets with graph cnn for network-scale traffic prediction. 2019 International Joint Conference on Neural Networks (IJCNN), pages 1–8, 2019.

[88] S. Zhao, Y. Wang, B. Li, B. Wu, Y. Gao, P. Xu, T. Darrell, and K. Keutzer. epointda: An end-to-end simulation-to-real domain adaptation framework for lidar point cloud segmentation. In AAAI Conference on Artificial Intelligence, 2020.

[89] J.-Y. Zhu, T. Park, P. Isola, and A. Efros. Unpaired image-to-image translation using cycle-consistent adversarial networks. pages 2242–2251, 10 2017.

[90] V. Zyrianov, X. Zhu, and S. Wang. Generate realistic lidar point clouds. In Computer Vision – ECCV 2022: 17th European Conference, Tel Aviv, Israel, October 23–27, 2022, Proceedings, Part XXIII, page 17–35, Berlin, Heidelberg, 2022. Springer-Verlag.

Hamed Haghighi is a PhD candidate with the Warwick Manufacturing Group (WMG) at the University of Warwick, UK. He received a B.Sc. (2016) in Software Engineering from the Isfahan University of Technology (Isfahan, Iran) and an M.Sc. (2019) in Artificial Intelligence from the University of Tehran (Tehran, Iran). His research interests include machine learning, computer vision, computer graphics, and autonomous vehicles.

Xiaomeng Wang Dr Xiaomeng Wang received a B.S. degree in Communication Engineering and an MSc degree in Information Engineering from Communication University of China in 2010 and 2013 respectively, and a PhD degree in Computer Science from the Computer Vision Laboratory at the University of Nottingham in 2018. Xiaomeng has worked as a research associate at the Graphics & Interaction Group in the Department of Computer Science and Technology, University of Cambridge, from 2017 to 2019. She is currently a research fellow in the Intelligent Vehicle Group at WMG, University of Warwick. Her main research interests involve computer vision, machine learning, and their applications.

Hao Jing Dr Hao Jing is currently a Senior Research Fellow in the Intelligent Vehicle Group at WMG, University of Warwick, with a research focus on high-performance integrated and cooperative vehicle positioning and navigation solutions in challenging environments. Dr Jing previously completed her PhD at the University of Nottingham on the topic of collaborative indoor positioning. She has worked on several projects that focus on achieving reliable and robust navigation performance for Connected and Autonomous Vehicles (CAV), pedestrians and mobile mapping systems in various environments and scenarios, based on solutions that make use of GNSS, Lidar, IMU and wireless signals.

Mehrdad Dianati Professor Mehrdad Dianati leads Networked Intelligent Systems (Cooperative Autonomy) research at Warwick Manufacturing Group (WMG), University of Warwick. He has over 28 years of combined industrial and academic experience, with 20 years in leadership roles in multidisciplinary collaborative R&D projects, in close collaboration with the Automotive and ICT industries. He is also the Co-Director of Warwick's Centre for Doctoral Training on Future Mobility Technologies, training doctoral researchers in the areas of intelligent and electrified mobility systems in collaboration with the experts in the field of electrification from the Department of Engineering of the University of Warwick. In the past, he served as an associate editor for the IEEE Transactions on Vehicular Technology and several other international journals, including IET Communications. Currently, he is the Field Chief Editor of Frontiers in Future Transportation. His academic experience includes over 25 years of teaching undergraduate and post-graduate level courses and supervision of research students. He currently leads a post-graduate course in Machine Intelligence.